JVST B
Journal of Vacuum Science & Technology B

# Thermochemical prediction of runaway energetic reactions involving organometallic (Al, In) and silane precursors in deposition tools

Cite as: J. Vac. Sci. Technol. B **40**, 012201 (2022); https://doi.org/10.1116/6.0001503
Submitted: 28 September 2021 • Accepted: 12 November 2021 • Published Online: 06 December 2021

**Yicheng Liu, Norleakvisoth Lim, Taylor Smith, et al.**

JVST B
Journal of Vacuum Science & Technology B

ARTICLE

avs.scitation.org/journal/jvb

# Thermochemical prediction of runaway energetic reactions involving organometallic (Al, In) and silane precursors in deposition tools

Cite as: J. Vac. Sci. Technol. B 40, 012201 (2022); doi: 10.1116/6.0001503
Submitted: 28 September 2021 · Accepted: 12 November 2021 ·
Published Online: 6 December 2021



Yicheng Liu,[1] Norleakvisoth Lim,[1] Taylor Smith,[1] Xia Sang,[2] and Jane P. Chang[1,2,a)]

## AFFILIATIONS

[1]Department of Chemical and Biomolecular Engineering, University of California, Los Angeles, Los Angeles, California 90095
[2]Department of Materials Science and Engineering, University of California, Los Angeles, Los Angeles, California 90095

[a)]**Electronic mail:** jpchang@ucla.edu

## ABSTRACT

In the manufacturing of integrated circuits (ICs), many deposition systems use solid, liquid, and gaseous precursors that can form potentially hazardous by-products in the exhaust lines. To assess the likelihood of an energetic reaction taking place, Gibbs free energy minimization was used to examine the reactions between chemical precursors, such as trimethylaluminum, trimethylindium, silane, and silane derivatives with $H_2O$, $O_3$, and $Cl_2$. For the trimethyl-metal precursors, $CH_4$ is a major by-product in both the $O_3$ and $H_2O$ environments, and $CH_4$, HCl, and $CCl_4$ are possible products in the $Cl_2$ environment. For silanes, a small $H_2O$ to silane ratio leads predominantly to the formation of $H_2$ and siloxane while a large $H_2O$ to silane ratio leads primarily to the formation of $H_2$ and more $H_2O$. In addition to depositing reaction by-products, unreacted precursors may also deposit on the interior surfaces of the exhaust system, narrowing the cross-sectional area of the pipes. These narrowed regions can become temperature, pressure, and concentration hot spots where energetic reactions are more likely to occur. Results from this analysis may be helpful in designing a safer downstream exhaust system that minimizes the risk of energetic events.



## I. INTRODUCTION

Over the past decade, the percentage of integrated circuits (ICs) manufactured in the United States has been sharply declining. It is reported that the percentage of U.S.-manufactured semiconductors sharply decreased from 37% in 1990 to 12% in 2020.[1] However, recent developments suggest that domestic manufacturing may increase with more industrial and federal investment.[2,3] As fabs are built and expanded across the United States, operation safety will again be a primary concern.

Maintaining a safe working environment is complicated by the wide variety of chemicals used. As microelectronic devices have become more complex, many new materials have been adopted. Thus, novel deposition precursors are being developed and implemented for chemical vapor deposition (CVD) and atomic layer deposition (ALD) processes. For example, trimethylindium (TMIn) has been used for depositing InN and $In_2O_3$,[4–7] trimethylaluminum (TMA) for Al and $Al_2O_3$,[8,9] and silane and its derivatives for Si and $SiO_2$.[10,11] These reactive precursors raise many safety concerns, including the possibility of energetic events, such as fires and explosions. Although these energetic events can occur in many locations, data from 2010 to 2013 indicate that the vast majority occurred downstream of the tool in the exhaust lines.[12]

Several incidents involving energetic events of reactive precursors have been reported in IC manufacturing plants. In 2013, a fatality resulted from a fire caused by TMIn being exposed to air.[13] Three years later at the same facility, a mechanical failure exposed TMA to air, resulting in an explosion that hospitalized four people.[14] In 1995, disilane accumulated in the downstream section and came in contact with air at damaged piping, resulting in unexpected combustion and injuries. Two fires at semiconductor fabs originating from small chemical fires in 1996 and 1997 caused losses of $\$220 \times 10^6$ and $\$470 \times 10^6$, respectively, highlighting the economic costs associated with energetic events.[15]

In spite of their risks, these precursors are still used due to their effectiveness. Thus, to prevent similar energetic events, many Environmental, Health and Safety (EHS) departments have

implemented guidelines for the use of energetic materials in the semiconductor industry.[16] The pyrolysis of reactive precursors is vital to potential energetic events. Computational studies have been conducted to understand the reactions involving pyrolysis of certain precursors, such as TMIn,[17] TMA,[18] and silane.[19] In addition, models of the exhaust systems have been made to determine how temperature, concentration, and solid buildups may occur along the length of the exhaust lines.[20]

Table I presents potential hazards related to TMIn, TMA, and silane. These particular chemicals were selected to demonstrate how precursors in the solid (TMIn), liquid (TMA), and gaseous (silane) phases at STP can each lead to hazardous conditions. These precursors' ability to undergo pyrolysis makes them particularly dangerous and necessitates extra caution. Not only are they flammable in contact with air, but their by-products also pose risks. Solid by-products can restrict exhaust lines, potentially forming hot spots. Liquid by-products can accumulate in locations such as capped tees until they reach dangerous concentrations. Gaseous by-products may interact with each other in the exhaust lines, leading to energetic events. Thus, determining what products are formed and are present in the exhaust system is of vital importance to prevent or mitigate these energetic events.

Three gaseous compounds that are commonly seen in exhaust systems are selected for evaluation with the chemical precursors listed above: $H_2O$, $O_3$, and $Cl_2$. $H_2O$ is a commonly used precursor in ALD, and $O_3$ is often used as a source of atomic O. $Cl_2$ is used in various IC fabrication processes and can be in the exhaust system.

Gibbs free energy minimization is a common technique used to determine thermodynamically favored products.[21–25] Although this technique does not account for the effects of kinetics, techniques such as blocking exist to exclude kinetically unfavorable products from the calculations. In this work, Gibbs free energy minimization is used to predict the by-products of deposition processes using organometallic compounds and silane precursors; examine the effects of pressure, temperature, and precursor concentrations on the formation of by-products; and determine potential risks posed by these systems.

## II. METHODS

The thermal equilibrium of a system at constant temperature and pressure can be determined by minimizing the total Gibbs free energy of the system, which is described by Eq. (1),

$$G(T, P, \{n_i\}^j) = \sum_{i=1}^{j} n_i \mu_i(T, P, \{n_i\}), \tag{1}$$

**TABLE I.** Safety information for reactive precursors obtained from MSDS.

| Precursor | STP form | $T_{bp}$ (°C) | $T_{mp}$ (°C) | Hazard |
|---|---|---|---|---|
| TMIn | Solid | 136 | 88 | Pyrophoric, corrosive, water-reactive |
| TMA | Liquid | 125 | 15 | Pyrophoric, irritant, water-reactive |
| Silane | Gas | N/A | N/A | Pyrophoric, flammable |

where $n_i$ is the number of moles of species $i$, $\mu_i$ is the chemical potential of species $i$, and $j$ denotes the number of chemical species in the system.

The chemical potential of each species is described by Eq. (2),

$$\mu_i = G_{fi}(T) + RTln\left(\frac{\hat{f}_i}{f_i^\circ}\right), \tag{2}$$

where $G_{fi}$ is the Gibbs free energy of formation of species $i$, $T$ is the temperature, $R$ is the ideal-gas constant, $\hat{f}_i$ is the fugacity of species $i$ in the system, and $f_i^\circ$ is the fugacity of pure species $i$ at its ideal-gas standard state, which is equivalent to $P^0$.

The gaseous species is assumed to be ideal because the pressure range employed in this study is from $10^{-5}$ to 1 atm. The fugacity for gaseous species, $\hat{f}_i^g$, can be described by Eq. (3). In addition, solids and liquids in the system are assumed to be incompressible. The fugacity for the condensed phases, $\hat{f}_i^{s,l}$, is represented by Eq. (4),

$$\hat{f}_i^g = y_i \phi_i P, \tag{3}$$

$$\hat{f}_i^{s,l} = P_i^{sat} \exp[B_{ii} P_i^{sat} + V_i^{s,l}(P - P_i^{sat})], \tag{4}$$

where $y_i$ is the mole fraction of species $i$, $\phi_i$ is the fugacity coefficient of species $i$, $P$ is the system pressure, $P_i^{sat}$ is the saturation pressure of species $i$, and $V_i^{s,l}$ is the molar volume of species $i$. $B_{ii}$ is the second virial coefficient for species $i$, which is neglected under the ideal gas assumption.

The chemical potentials for gaseous species and condensates are shown in Eqs. (5) and (6), respectively,

$$\mu_i^g = G_{fi}(T) + RTln\left(\frac{y_i P}{P^\circ}\right), \tag{5}$$

$$\mu_i^{s,l} = G_{fi}(T) + RTln\left(\frac{P^{sat}}{P^\circ}\right) + RTV_i^{s,l}(P - P^{sat}). \tag{6}$$

The conservation of atomic masses is used as a constraint in the calculation. The minimization problem of the total Gibbs free energy of the system is presented in Eq. (7),

$$\left\{ \begin{array}{c} \min\limits_{\{n_i\}_{i=1}^j} (G(T,\ P,\ \{n_i\}_{i=1}^j)) \\ Constraint: \sum\limits_i n_i a_{ik} - A_k = 0 \\ (k = 1,\ 2,\ \ldots,\ l) \end{array} \right\}, \tag{7}$$

where $n_i$ is the number of moles of species $i$, $a_{ik}$ is the number of atoms of element $k$ in species $i$, $A_k$ is the total number of moles of element $k$ in the system, and $l$ denotes the total number of elements.

The HSC Chemistry[21,22,24,26] database provided the thermochemical data and physical properties of chemical species considered for the following precursors: TMIn, TMA, silane, and various chlorosilanes ($SiH_3Cl$, $SiH_2Cl_2$, and $SiHCl_3$). Calculations were

performed to see how these precursors would react with $H_2O$, $O_3$, and $Cl_2$.

Although the HSC database contains many of the possible reaction products, there are some products reported in the literature that are not available in the HSC database. In these cases, equilibrium concentrations were calculated first using only the data in the HSC database, and then thermochemical data for species taken from literature sources[26–29] were added to the calculation. This allowed for the comparison of the equilibrium with and without those compounds.

Thermodynamic calculations such as Gibbs free energy minimization do not take kinetic factors into account. Thus, thermodynamic calculations could suggest the formation of a particular stable product, but its formation could be prevented by kinetic barriers. To resolve these discrepancies, species that are favored thermodynamically but that are not observed experimentally can be removed from the thermodynamic calculations, simulating impenetrable kinetic barriers. This technique is sometimes referred to as blocking. However, care must be taken when applying this method, as often these kinetic barriers are not infinite and this assumption can lead to conflicts with experimental data.[21]

Using data from the HSC database, the equilibrium concentrations of the various reaction products were determined at a temperature range from 0 to 500 °C; pressures of $10^{-5}$, $10^{-2}$, and 1 atm; and starting composition ratios of 1:1 and 1:100. The calculations were repeated including data that were reported in the literature but not included in the HSC database. The blocking technique was also applied to possible products to demonstrate the effect that kinetically unfavorable reactions can have on a system.

Results for TMIn and silane are reported in the body of this paper. See supplementary material for results of TMA (Figs. S1 and S2), disilane (Fig. S3), and dichlorosilane (Fig. S4).[33]

## III. TMIn RESULTS AND DISCUSSION

The various reaction pathways for TMIn are shown in Fig. 1. The first step of all reactions is the heating of TMIn to form a gaseous phase. TMIn is a useful precursor for $In_2O_3$ specifically because of its relatively high vapor pressure compared to other indium precursors.[7] The gaseous TMIn can then be pyrolyzed as shown in section (I) of Fig. 1 to form $In(CH_3)_2(g)$ and $CH_3(g)$. Ott *et al.* noted that this pyrolysis occurs at temperatures above 252 °C.[4] $CH_3$ groups can be further removed to form $InCH_3(g)$ and In(s). The removed $CH_3$ can react with gaseous TMIn to form methane ($CH_4$) and $In(CH_3)_2CH_2(g)$. Upon heating, methane can decompose to form $H_2$ gas and deposit carbon. Additionally, methyl radicals can react with each other to form ethane ($C_2H_6$).

Section (II) of Fig. 1 shows how in the presence of $H_2O$, gaseous $In(CH_3)_3$ reacts to form methane and $In(OH)_3$. The hydroxides undergo a dehydration reaction at high temperatures to form $In_2O_3(s)$ and $H_2O$. $In_2O_3$ can then react with the solid carbon deposits to form liquid indium and CO(g).

In the presence of $Cl_2$, there are two main reaction pathways. As shown in section (III), the first reaction with $Cl_2$ occurs with methane and forms $CCl_4(g)$ and HCl(g). Upon heating, $CCl_4$ can decompose to form $Cl_2$ and a solid carbon deposit. This second reaction pathway is illustrated in section (IV) of Fig. 1. Section (IV) of Fig. 1 shows the second reaction pathway in which atomic Cl can react with liquid indium to form InCl(g). InCl(g) can then react with an additional Cl atom to form $InCl_2(s)$, which can react with itself to form $In_2Cl_4(g)$. $In_2Cl_4(g)$ can then decompose into $InCl_3(l)$ and InCl(g).

In an $O_3$ environment, $O_3$ first decomposes into $O_2(g)$ and atomic O(g). In the presence of $O_2$, ethane and methane formed from TMIn pyrolysis can undergo combustion reactions to form $CO_2(g)$ and $H_2O(g)$. $O_2(g)$ can also oxidize the indium formed from TMIn pyrolysis. Additionally, atomic O(g) can react with $In(CH_3)_3$ to form $In(OH)_3(s)$ and $CH_2O(g)$. As in the $H_2O$ environment, dehydration of indium hydroxides can also occur at high temperatures. Because $H_2O$ has been formed, possible reactions at this point are similar to those of the pure $H_2O$ system.

Table II shows the heats of reaction at 298 K for the dominant reactions found in the TMIn system. Heats of reaction were calculated from heats of formation in the HSC database. Data for heats of formation not found in the HSC database were obtained from Skulan *et al.*[28]

The thermodynamically favored products for the TMIn-$H_2O$ and the TMIn-$Cl_2$ systems at 1 atm and in the range of 100–300 °C are shown in Table III. This temperature range was selected because typical temperatures for deposition of $In_2O_3(s)$ via CVD are between 100 and 300 °C.[4,6,7] Analysis for other temperature and pressure ranges was also performed and can be found in Table S1.[33] Table III shows not only the effects of switching gases from $H_2O$ to $Cl_2$ but also the effects of changing the starting ratios of TMIn to the other reactant gas. Also shown in Table III are the TMIn-$H_2O$ systems if CO and $CO_2$ are either included or suppressed as possible reaction products. Although this did not have any effect on the 1:1 system, blocking CO and $CO_2$ formation led to the deposition of C in the 1:100 system.

If the heats of formation from the literature for TMIn and other species like $In(CH_3)_3$ were included, no change occurred at 1 atm and in the range of 100–300 °C. However, excluding them from the calculations at 1 atm and 0–100 °C added TMIn as a product gas and removed In(s) and C(s) as deposition products. This discrepancy highlights the importance of being selective about which data to use as inaccurate data may lead to erroneous determination of which species are in the system.

Table III also highlights one of the primary challenges of working with TMIn, namely, that all reaction pathways lead to flammable or highly corrosive products. The exothermic reactions involved in the system and shown in Table II emphasize the dangers of having flammable species in the exhaust systems downstream of the reaction chambers. Energetic reactions such as the formation of $In(OH)_3$ can lead to the ignition of the highly flammable species. Dangerous by-products and unreacted precursor molecules can be removed from the exhaust line with an appropriate abatement system.[30]

Additionally, the ratios of $Cl_2$, $H_2O$, and $O_3$ can alter the most favorable product. In the In-$H_2O$ system, reducing the amount of $H_2O$ in the system to a 1:1 ratio eliminated the formation of $In(OH)_3$. The deposition of $In(OH)_3$ is a very exothermic process (Table II), so reducing its deposition by lowering the amount of $H_2O$ in the system could potentially reduce the risk of an energetic event. Likewise, limiting the deposition of $In(OH)_3$ in the exhaust

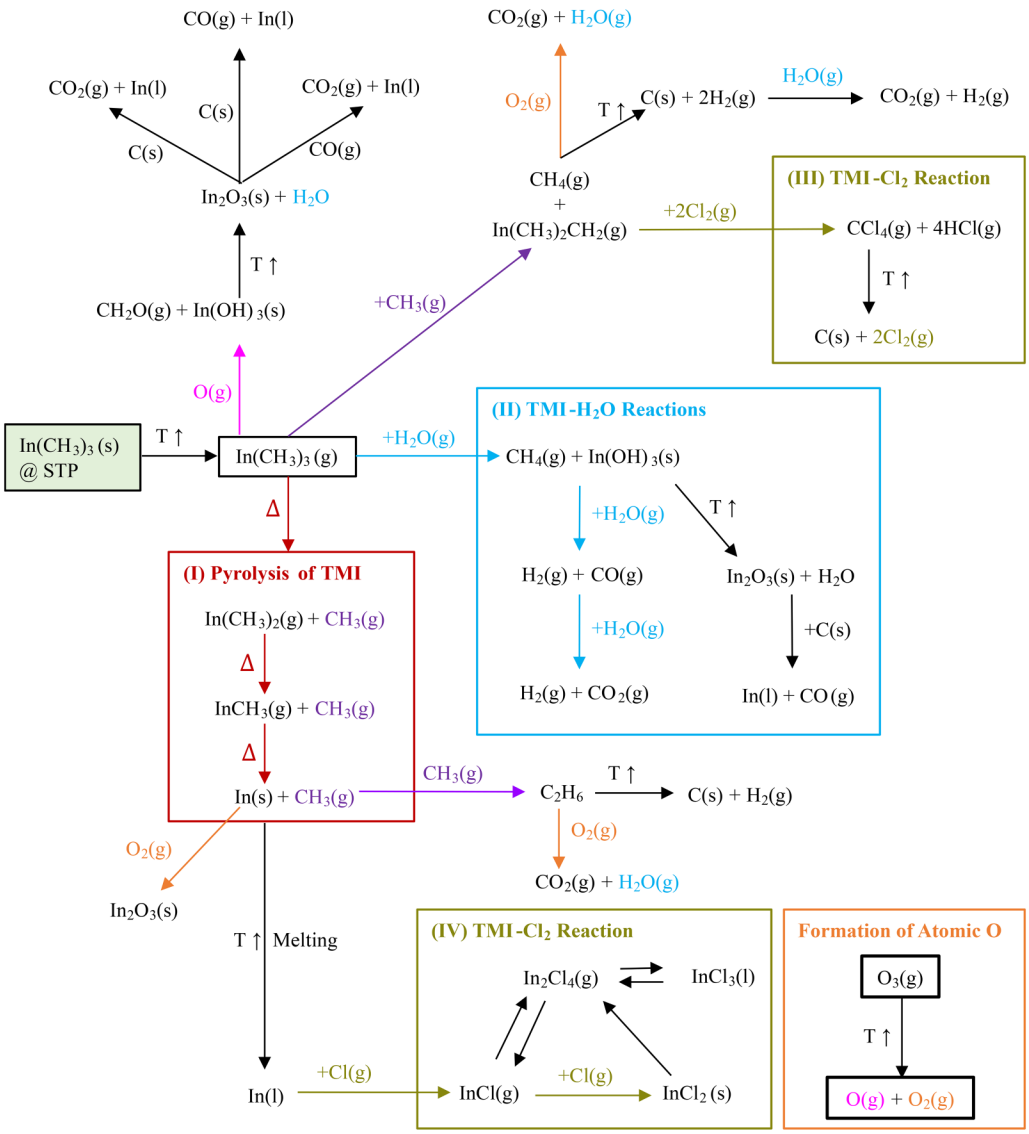


**FIG. 1.** Possible reactions of a TMIn system. (I) Pyrolysis reactions of TMIn. (II) $H_2O(g)$ reactions with TMIn. (III) First set of $Cl_2$ reactions with TMIn. (III) Second set of $Cl_2$ reactions with TMIn.

lines can prevent the cross section of the exhaust line from being reduced. Reductions in the cross section can lead to the buildup of pressure, temperature, and potentially flammable by-products in the exhaust line, increasing the risk of an energetic event.

The effects of temperature and pressure were also examined for the 1:1 TMIn:$H_2O$ system. Figure 2(a) shows these results for indium if only data from the HSC database are used. Solid indium is formed at temperatures below the melting point of 156.6 °C, above which all indium is in the liquid phase. However, the amount of indium produced at low temperatures in this scenario decreases quickly to zero at atmospheric pressure. Figure 2(b) shows the results if the data from Skulan *et al.* are included.[28] In this case, solid indium is deposited even at the lowest temperatures examined. Regardless of whether the data from the literature are included, there is a dramatic increase in the amount of liquid indium produced at high temperatures, likely due to the dominance of the pyrolysis reaction pathways at high temperatures.[4,6] As shown in Fig. 1, the main product of the pyrolysis pathway in the absence of $O_2(g)$ is solid or liquid indium.

Although the differences in this case do not appear large, the differences between Figs. 2(a) and 2(b) illustrate the potential limitations of using data from only the HSC database. If the database

**TABLE II.** Heats of reaction of dominant reactions in the TMIn system.

| Dominant reaction | $\Delta H_{298K}$ (kcal mol$^{-1}$) |
|---|---|
| $2In(OH)_3(s) \rightarrow In_2O_3(s) + 3H_2O(g)$ | 43.20 |
| $In(CH_3)_3(g) \rightarrow In(CH_3)_2(g) + CH_3(g)$ | 64.30 |
| $InCH_3(g) \rightarrow In(s) + CH_3(g)$ | −12.8 |
| $In(CH_3)_3(g) + H(g) \rightarrow InCH_3(g) + CH_4(g) + CH_3(g)$ | −40.99 |
| $CH_4(g) \rightarrow C(s) + 2H_2(g)$ | 17.83 |
| $O_3(g) \rightarrow O_2(g) + O(g)$ | 25.66 |
| $In(CH_3)_3(g) + 6O(g) \rightarrow In(OH)_3(s) + CH_2O(g)$ | −672.94 |
| $C(s) + 2H_2O(g) \rightarrow CO_2(g) + 2H_2(g)$ | 21.55 |

does not contain species of interest, calculations may be inaccurate. However, this can be corrected by including appropriate data from experiments or modeling.

## IV. SILANE RESULTS AND DISCUSSION

The reactions involving silane are shown in Fig. 3. The boiling point of silane is −112 °C, so there is no need to include the liquid phase.[31] For species that were not found in the HSC database, data were obtained from Allendorf *et al.*[29]

Silane can pyrolyze to eventually form a solid phase, as shown in section (I) of Fig. 3. This occurs as successive $H_2(g)$ molecules are formed with the application of heat. Pyrolysis of silane generally begins at approximately 370 °C.[32] Si(s) that is formed is then an important species in the formation of $SiO_2(s)$, as discussed below.

Water is an essential component of all reaction pathways for silane, as shown in Fig. 3. In a water-only system, Si(s) formed by the pyrolysis of silane reacts with $H_2O(g)$ to form $SiO_2(s)$ and $H_2(g)$. However, water can also react directly with silane yielding $H_2(g)$ and $SiH_3OH(g)$. From here, the resulting products depend largely on the ratio of $H_2O$ to $SiH_4$.

When the $H_2O$ to $SiH_4$ ratio is small, as shown in section (II) of Fig. 3, $SiH_3OH(g)$ can react with silane to form siloxane ($H_3SiOSiH_3$). Alternatively, it can react with another $SiH_3OH(g)$ molecule to form siloxane and $H_2O(g)$.

In an environment with high water vapor content, as shown in section (III) of Fig. 3, substitution of hydrogen with the hydroxyl groups in $SiH_3OH(g)$ forms $SiH_2(OH)_2(g)$, $SiH(OH)_3(g)$, and $Si(OH)_4(g)$. These can further decompose into $H_2O(g)$ and $Si(OH)_2O(g)$. A final decomposition can then occur, leading to the removal of $H_2O(g)$ and the formation of $SiO_2(s)$.

In an $O_3(g)$ environment, a critical reaction is the decomposition of $O_3(g)$ to form $O(g)$ and $O_2(g)$. The diatomic oxygen can oxidize Si(s) formed from the silane pyrolysis reaction to yield $SiO_2(s)$. The undecomposed $O_3(g)$ can also react with the silane precursor to form silanol ($H_3SiOH$) and $O_2(g)$. Decomposition reactions then follow a similar pathway as in the water-only environment, leading to the eventual formation of $Si(OH)_4(g)$ and $SiO_2(s)$, as shown in section (IV) of Fig. 3.

The major products for the silane reactions at 1 atm and in the range of 300–500 °C are shown in Table IV. This temperature range was selected based on deposition temperatures reported in the literature.[10,32] Results for additional temperature and pressure measurements are included in Table S2.[33]

**TABLE III.** Major products from the various reaction schemes for TMIn at 1 atm and in the temperature range of 100–300 °C.

| System | Exclude | Major gas | Deposition |
|---|---|---|---|
| $TMIn:H_2O = 1:1$ | | $CH_4$ | In(s), In(l), $In_2O_3$, C |
| $TMIn:H_2O = 1:1$ | $CO/CO_2$ | $CH_4$ | In(s), In(l), $In_2O_3$, C |
| $TMIn:H_2O = 1:100$ | | $CH_4$, $H_2O$ | $In(OH)_3$, $In_2O_3$ |
| $TMIn:H_2O = 1:100$ | $CO/CO_2$ | $CH_4$, $H_2O$ | $In(OH)_3$, $In_2O_3$, C |
| $TMIn:O_3 = 1:1$ | | $CH_4$, $H_2O$ | $In_2O_3$, C |
| $TMIn:Cl_2 = 1:1$ | | $CH_4$ | C, $InCl_2$ |
| $TMIn:Cl_2 = 1:100$ | | $Cl_2$, $CCl_4$, HCl | $InCl_3$ |

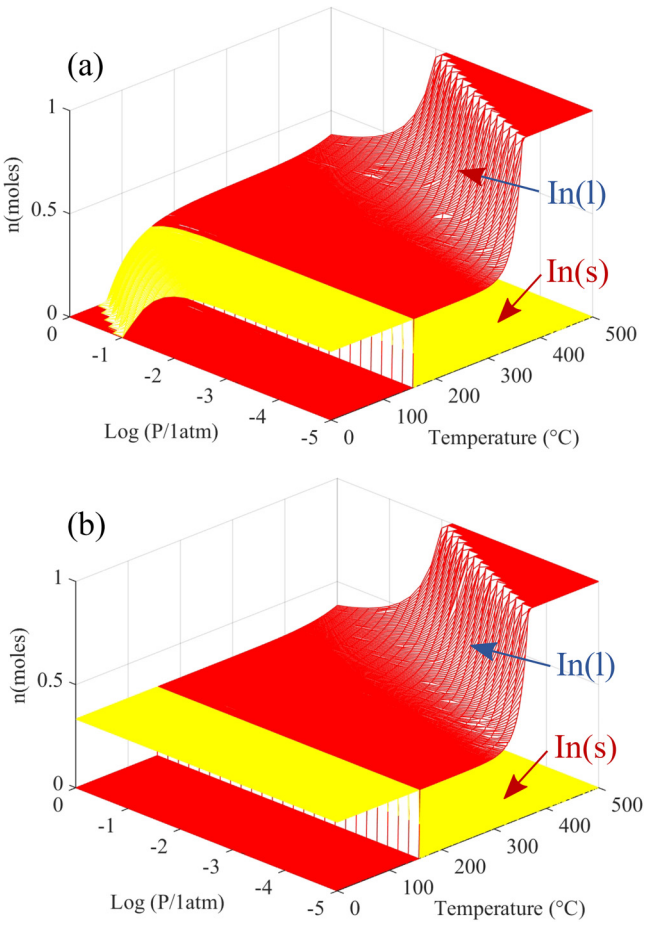


**FIG. 2.** Indium formed as a function of temperature and pressure based on calculations from (a) only the HSC database and (b) the HSC database and the data from Skulan *et al.*[28]

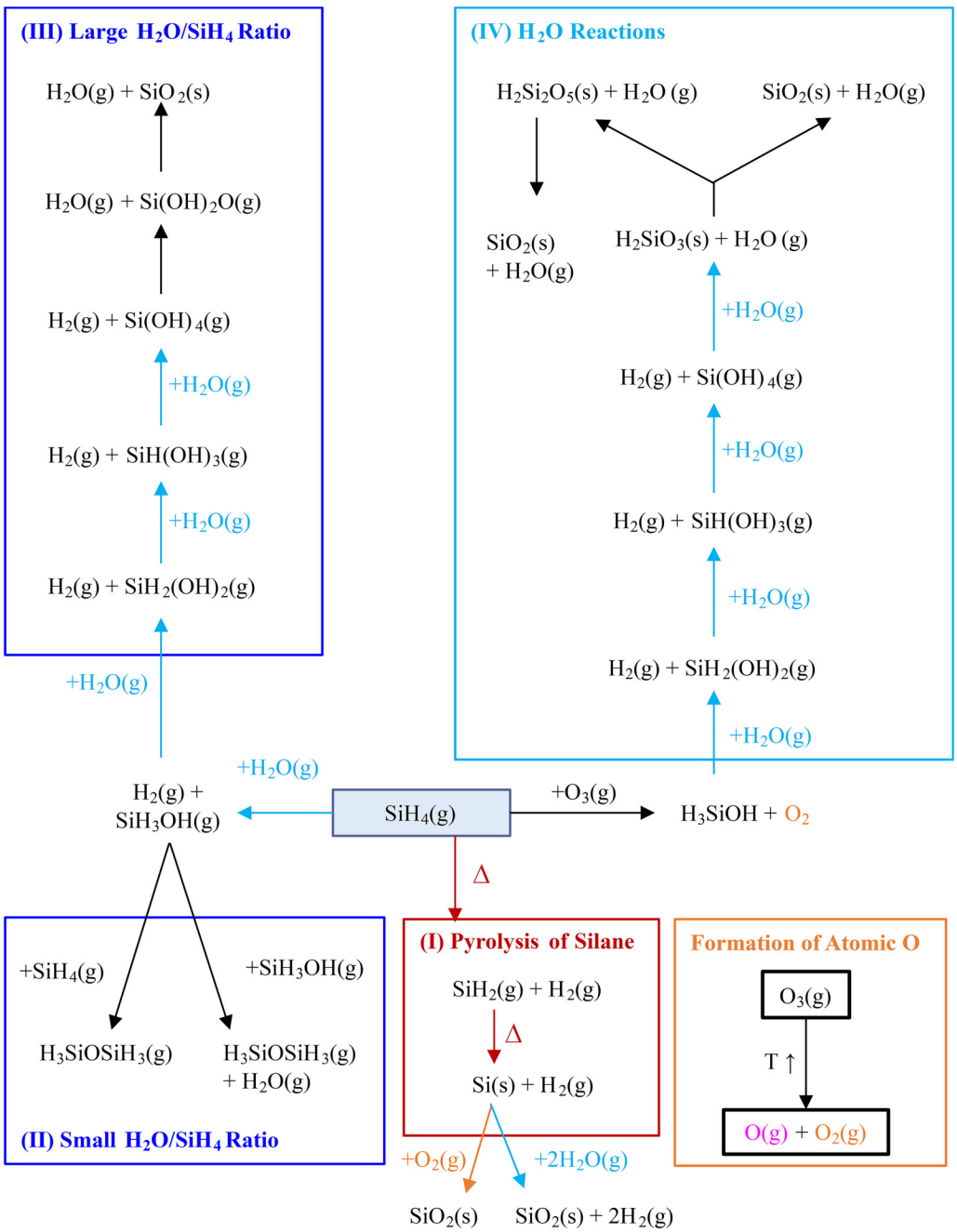


**FIG. 3.** Possible reactions for a silane system. (I) Pyrolysis reactions of silane. (II) Reactions between water and silane at low $H_2O$:$SiH_4$ ratios. (III) Reactions between water and silane at high $H_2O$:$SiH_4$ ratios. (IV) Reactions between water and $H_3SiOH$.

For the 300–500 °C temperature range, Table IV highlights $SiO_2$ as the major deposition product if it is kinetically favorable. Analysis was also done to determine the reaction products in the $O_3$ environment if $SiO_2$ deposition is kinetically unfavorable. In this case, the major reaction products were determined to be $H_2Si_2O_5$ and $H_2SiO_3$.

Table IV shows that silane reactions form $H_2(g)$ under several different operating conditions, leaving the extremely flammable gas

**TABLE IV.** Major products for the various silane reaction systems at 1 atm and in the temperature range of 300–500 °C.

| System | Exclude | Major gas | Deposition |
|---|---|---|---|
| $SiH_4$:$H_2O$ = 1:1 | | $H_2$, $H_3SiOSiH_3$ | $SiO_2$ |
| $SiH_4$:$H_2O$ = 1:100 | | $H_2$, $H_2O$ | $SiO_2$ |
| $SiH_4$:$O_3$ = 1:1 | | $H_2$, $H_2O$ | $SiO_2$ |
| $SiH_4$:$O_3$ = 1:1 | $SiO_2$ | $H_2$, $H_2O$ | $H_2Si_2O_5$, $H_2SiO_3$ |
| $SiH_4$:$O_3$ = 1:100 | | $O_2$, $H_2O$ | $SiO_2$ |
| $SiH_4$:$O_3$ = 1:100 | $SiO_2$ | $O_2$, $H_2O$ | $H_2Si_2O_5$, $H_2SiO_3$ |

in the exhaust. Even when $H_2$ does not form in the silane system, $O_2$ is still produced, which as an oxidizer can cause other energetic events to be much more dangerous and even explosive.

Another issue highlighted by the results is the formation of several solid deposits. These deposits can cause various issues in the exhaust system. For example, they can deposit on the interior of the exhaust walls, reducing the line diameter. This constricted diameter may lead to spikes in temperature, pressure, and concentration. These risks can be mitigated by using an appropriate scrubbing system to remove solid particles and prevent them from building up.[15] Regular preventative maintenance can also be scheduled to remove any solid buildup.

With the $SiH_4$-$O_3$ system, the ratio of precursor to $Cl_2$, $H_2O$, or $O_3$ also has an important effect on the product species. Including large amounts of $O_3$ can help limit the formation of highly flammable $H_2$ gas, although it leads to the formation of $O_2$, which can be dangerous if other flammable species are present in line. Likewise, a small $H_2O$:silane ratio can increase the amount of siloxane produced and decrease the formation of $H_2$.

Table V compares the dominant gas and deposition species that are present when using silane and chlorosilane precursors at a 1:1 ratio with $H_2O$. $H_2$ is a thermodynamically favorable product for any silane precursor that contains H atoms and is only eliminated when $SiCl_4$ is used as the precursor.

There were several key differences between the trimethyl metallic chemistries and the silane chemistries. Both chemistries could produce $H_2$, and $H_2O$; however, the trimethyl chemistries were capable of forming CO and $CO_2$ while the silane chemistries could form siloxane. Unless $SiO_2$ was excluded, silane deposited only Si and $SiO_2$, while the trimethyl chemistries produced metals, oxides, and hydroxides. As mentioned earlier, the hydroxide formation is of particular concern due to its large exothermic heat of reaction. Carbon deposits could also form in the trimethyl chemistries, as shown when the pathways to form CO and $CO_2$ were considered blocked by infinite kinetic barriers and removed from the possible products.

**TABLE V.** Summary of reactions of chlorinated silane with $H_2O$ at a molar ratio of 1:1.

| Precursor | Major gas | Deposition |
|---|---|---|
| $SiH_4$ | $H_2$, $H_3SiOSiH_3$ | Si, $SiO_2$ |
| $SiH_3Cl$ | $H_2$, $SiCl_4$, $SiHCl_3$ | Si, $SiO_2$ |
| $SiH_2Cl_2$ | $H_2$, $SiCl_4$ | $SiO_2$ |
| $SiHCl_3$ | $H_2$, $SiCl_4$, HCl | $SiO_2$ |
| $SiCl_4$ | $SiCl_4$, HCl | $SiO_2$ |

## V. SUMMARY

In the TMIn system, highly flammable methane was formed in almost all conditions at atmospheric pressure and between 100 and 300 °C. The only exception was the 1:100 TMIn:$Cl_2$ system, which still produced dangerous $CCl_4$ and HCl. Likewise, silane produced dangerous by-products in both $H_2O$ and $O_3$ at 1 atmosphere and in the temperature range of 300–500 °C. $H_2$ is formed regardless of the $H_2O$ to silane ratio, but small ratios lead to the formation of siloxane and a reduction in the amount of $H_2$ produced. On the other hand, large $H_2O$:silane ratios strongly favor the formation of $H_2$, with additional $H_2O$ also being formed. In an ozone environment, the silane reacts to form $O_2$ and $H_2O$. The $H_2$ produced is dangerous due to its flammability, while $O_2$ is an oxidizer and can increase the severity of other energetic events. All conditions considered also showed the formation of solid deposits including indium, $In_2O_3$, $In(OH)_3$, indium chlorides, carbon, $SiO_2$, $H_2Si_2O_5$, and $H_2SiO_3$, which could clog exhaust lines, create temperature and pressure hot spots, and increase the risk of energetic events. Some conditions also formed liquid phase by-products, which can accumulate at various points in an exhaust system until they build up to dangerous concentration levels.

Knowing which products are formed and which energetic reactions occur can improve awareness of possible dangerous events. When determining the various equilibrium concentrations, the source and quality of the data can have significant impact on the final results. Although thermodynamically favorable products can be determined using the method outlined in this work, the actual by-products may be different due to kinetics. Data about which products are actually formed are often closely guarded as intellectual property, limiting the effectiveness of this study. Nevertheless, this paper has demonstrated that blocking kinetically unfavorable products can effectively mimic kinetic effects. Thus, users with experimental data can apply the approach outlined in this paper to other chemical systems to determine which by-products will be present in their systems and incorporate appropriate safety measures.

## ACKNOWLEDGMENTS

The authors acknowledge financial support from the Semiconductor Research Corporation (No. 2018-006). This work was part of a joint project with Farhang Shadman's group at the University of Arizona. The authors acknowledge Texas Instruments for providing fab-safety-related basic information. The authors thank Caitlyn Chen and Owen Watkins for helping prepare the figures and tables.

## DATA AVAILABILITY

The data that support the findings of this study are available from the corresponding author upon reasonable request.

## REFERENCES

[1]A. Varas, J. Goodrich, R. Varadarajan, and F. Yinug, "Government incentives and U.S. competitiveness in semiconductor manufacturing," Boston Consulting Group (2020).
[2]A. Tilley, "Intel sets strategy to speed its chip revival," Wall Street Journal, March 24, 2021.
[3]A. Leary and P. Ziobro, "U.S. chip sector set to get $50 billion," Wall Street Journal, April 1, 2021.
[4]A. W. Ott, J. M. Johnson, J. W. Klaus, and S. M. George, Appl. Surf. Sci. **112**, 205 (1997).
[5]P. Deminskyi, P. Rouf, I. G. Ivanov, and H. Pedersen, J. Vac. Sci. Technol. A **37**, 020926 (2019).
[6]D.-J. Lee, J.-Y. Kwon, J. I. Lee, and K.-B. Kim, J. Phys. Chem. C **115**, 015384 (2011).
[7]A. U. Mane, A. J. Allen, R. K. Kanjolia, and J. W. Elam, J. Phys. Chem. C **120**, 9874 (2016).
[8]Z. Shi, P. Lu, and A. V. Walker, Langmuir **28**, 016909 (2012).
[9]Y.-I. Ogita, S. Iehara, and T. Tomita, Thin Solid Films **430**, 161 (2003).
[10]S. M. Gates, C. M. Greenlief, S. K. Kulkarni, and H. H. Sawin, J. Vac. Sci. Technol. A **8**, 2965 (1990).
[11]F. Gaillard, P. Brault, and P. Brouquet, J. Vac. Sci. Technol. B **14**, 2767 (1996).
[12]S. Trammell and A. McIntyre, "Environmental, safety, and health aspects of R&D and manufacturing with advanced processing materials," SEMATECH, Inc.
[13]"FATALITY Dow Chemical worker dies from burns sustained in fire at electronic materials facility," Chemical & Engineering News Archive 2013/10/21, 2013, p. 7.
[14]Z. Mathews, "Mechanical failure caused Dow Chemical explosion," The Eagle-Tribune, January 21, 2021.
[15]J. R. Chen, Process Saf. Prog. **21**, 19 (2002).
[16]SEMI, SEMI S30—Safety guideline for use of energetic materials in semiconductor R&D and manufacturing processes.
[17]A. H. McDaniel and M. D. Allendorf, Chem. Mater. **12**, 450 (2000).
[18]J. Slaughter, A. J. Peel, and A. E. H. Wheatley, Chem. Eur. J. **23**, 167 (2017).
[19]S.-W. Hu, Y. Wang, X.-Y. Wang, T.-W. Chu, and X.-Q. Liu, J. Phys. Chem. A **108**, 1448 (2004).
[20]E. Watson and F. Shadman, Int. J. Emerging Technol. Adv. Eng. **10**, 62 (2020).
[21]J. Acker and K. Bohmhammel, J. Organomet. Chem. **693**, 2483 (2008).
[22]M. L. Contreras, J. M. Arostegui, and L. Armesto, Fuel **88**, 539 (2009).
[23]K. C. Kim, M. D. Allendorf, V. Stavila, and D. S. Sholl, Phys. Chem. Chem. Phys. **12**, 9918 (2010).
[24]H. Tang and K. Kitagawa, Chem. Eng. J. **106**, 261 (2005).
[25]J. K.-C. Chen, T. Kim, N. D. Altieri, E. Chen, and J. P. Chang, J. Vac. Sci. Technol. A **35**, 031304 (2017).
[26]A. Roine, HSC chemistry for windows, 7.193, Outotec Research (2009).
[27]M. D. Allendorf, C. F. Melius, B. Cosic, and A. Fontijn, J. Phys. Chem. A **106**, 2629 (2002).
[28]A. J. Skulan, I. M. B. Nielsen, C. F. Melius, and M. D. Allendorf, J. Phys. Chem. A **110**, 281 (2006).
[29]M. D. Allendorf, C. F. Melius, P. Ho, and M. R. Zachariah, J. Phys. Chem. **99**, 015285 (1995).
[30]L. Mendicino, V. Vartania, B. Goolsby, P. T. Brown, and K. Reid, in *Environmental Issues with Materials and Processes for the Electronics and Semiconductor Industries*, edited by L. Mendicino (The Electrochemical Society, Inc., Pennington, NJ, 2001), pp. 68–77.
[31]P. J. Linstrom and W. G. Mallard, *NIST Chemistry Webbook* (National Institute of Standards and Technology, Gaithersburg, MD, 1997), NIST Standard Reference Database Number 69, p. 020899.
[32]P. Zhang, J. Duan, G. Chen, J. Li, and W. Wang, Sol. Energy **175**, 44 (2018).
[33]See supplementary material at https://www.scitation.org/doi/suppl/10.1116/6.0001503 for results of TMA, disilane and dichlorosilane.